



HAL
open science

Passive piezomagnetic monitoring of structures subjected to in-service cyclic loading: Application to the detection of fatigue crack initiation and propagation

A Ouaddi, O Hubert, J Furtado, D Gary, S He

► To cite this version:

A Ouaddi, O Hubert, J Furtado, D Gary, S He. Passive piezomagnetic monitoring of structures subjected to in-service cyclic loading: Application to the detection of fatigue crack initiation and propagation. *AIP Advances*, 2021, 11 (1), pp.015344. 10.1063/9.0000195 . hal-03124431

HAL Id: hal-03124431

<https://hal.science/hal-03124431>

Submitted on 28 Jan 2021

HAL is a multi-disciplinary open access archive for the deposit and dissemination of scientific research documents, whether they are published or not. The documents may come from teaching and research institutions in France or abroad, or from public or private research centers.

L'archive ouverte pluridisciplinaire **HAL**, est destinée au dépôt et à la diffusion de documents scientifiques de niveau recherche, publiés ou non, émanant des établissements d'enseignement et de recherche français ou étrangers, des laboratoires publics ou privés.

Passive piezomagnetic monitoring of structures subjected to in-service cyclic loading: Application to the detection of fatigue crack initiation and propagation

A. Ouaddi,^{1,2, a)} O. Hubert,¹ J. Furtado,² D. Gary,² and S. He³

¹⁾*Université Paris-Saclay, ENS Paris-Saclay, CNRS, LMT -
Laboratoire de Mécanique et Technologie, 91190 Gif-sur-Yvette,
France.*

²⁾*Air-liquide R&D, Innovation Campus Paris, 78354 Jouy-en-Josas Cedex,
France.*

³⁾*Léonard de Vinci Pôle Universitaire, Research Center, 92060 Paris La Défense,
France.*

(Dated: 28 January 2021)

In this research, the evolution of the piezomagnetic field of a low carbon steel under cyclic tensile stress was investigated. The objective was to explore the correlations between piezomagnetic signal measured by a fluxgate magnetometer with progressive changes that take place during the fatigue tests. Experiments show first that the piezomagnetic hysteresis loop changes drastically with the propagation of fatigue crack. A multiscale magneto-elastic model of the piezomagnetic behavior allows secondly the experimental cycles evolution to be explained.

^{a)}Electronic mail: achraf.ouaddi@airliquide.com.

I. INTRODUCTION

The application of a mechanical stress to a ferromagnetic material initially magnetized, even weakly, can lead to a variation of its magnetization. This is the so-called *Villari effect* or *piezomagnetic effect*¹⁻³. The magnetization variations depend on stress level, multiaxiality and rate, but also on the prior metallurgical-mechanical state of the material and its evolution in use. Its measurement can be done via a secondary coiling by measuring the induced voltage or via external magnetic flux gates, referred as leakage method in previous studies^{4,5}. Indeed, the magnetic flux leakage methods use the natural magnetization and its time evolution to investigate and characterize the structural integrity of structures.

In this study, the principle of passive monitoring by piezomagnetic variation of magnetic flux leakage in structures is first detailed. It is applied to monitor the propagation of a fatigue crack in a ferritic-pearlitic steel commonly used for pressure vessel construction. Results are then interpreted using a simplified magneto-elastic hysteresis model⁶.

II. MATERIAL AND EXPERIMENTAL PROCEDURE

The material used for the experiments is a C-Mn steel grade 42 with low carbon content (0.14%). It was machined from a pressure vessel construction which has been in service for many years. A fatigue test was executed on a pre-notched specimen (see figure 1 for design and dimensions) by applying a cyclic uniaxial mechanical loading. The main components of the experimental set up include an electronically controlled servohydraulic testing machine MTS-10T, two cameras (for displacement and strain measurement by Digital Image Correlation - DIC), a fluxgate magnetometer and a computer equipped with a National Instruments coprocessor board and a LabVIEW system for signal acquisition. The data sampling rate was 500 points per second. Magnetic flux signal (B-field) was measured by the fluxgate magnetometer. The magnetic sensor is a 1-axis fluxgate magnetometer (Fluxmaster #850 - Stefan Mayer Instruments) for the measurement of weak magnetic field (accuracy of $\pm 5nT$, range of $\pm 200\mu T$). It also permits to cancel out electronically the local ambient magnetic field. The magnetic probe has been mounted on a rigid non-magnetic stand which can move vertically along the specimen (Figure 2).

A sensitivity study about the optimal position of the magnetic probe suggested that the probe can be positioned closely and obliquely with respect to the specimen so that a relatively large

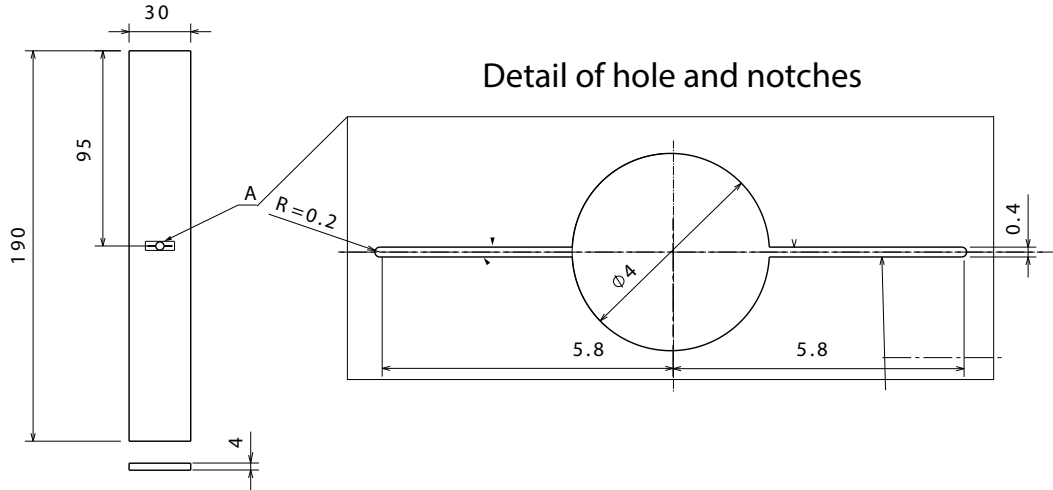


FIG. 1. Specimen: design and dimensions (mm).

variation in both the horizontal and normal components of the magnetic field could be measured. This study consists of measuring the variations of the magnetic field around the specimen at three different angles (45° , 90° and -45°) and at different positions. The specimen is not initially demagnetized. Results show that the B-field varies significantly around the specimen with localized maximal and minimal values, and its amplitude decreases drastically when moving away from the specimen (Figure 3). Given these results, the magnetic probe was placed about 10mm to specimen with an angle of 45° . Measurements were carried out at three different positions: at the level of the notch and ± 15 mm from this level in order to see how the signal varies with the position of the probe, expecting to avoid zero magnetic flux zones highlighted in figure 2 (NB: It has been verified that there was no significant relative movement between the probe and the specimen during the test).

A. Experimental details

The experiments were run under force control with sinusoidal profiles. The experimental procedure is iterative and includes three main steps:

1-Piezomagnetic measurement: at the beginning of the test and after each fatigue loading, a series of cyclic tensile loading were applied to the specimen. The B field and the mechanical loading were recorded during the loading process. The range of the applied force was [0kN - 18kN]. It was a 1Hz sinusoidal loading.

2-Fatigue loading: a series of 1000 sinusoidal cycles blocks each was performed (reduced to 500

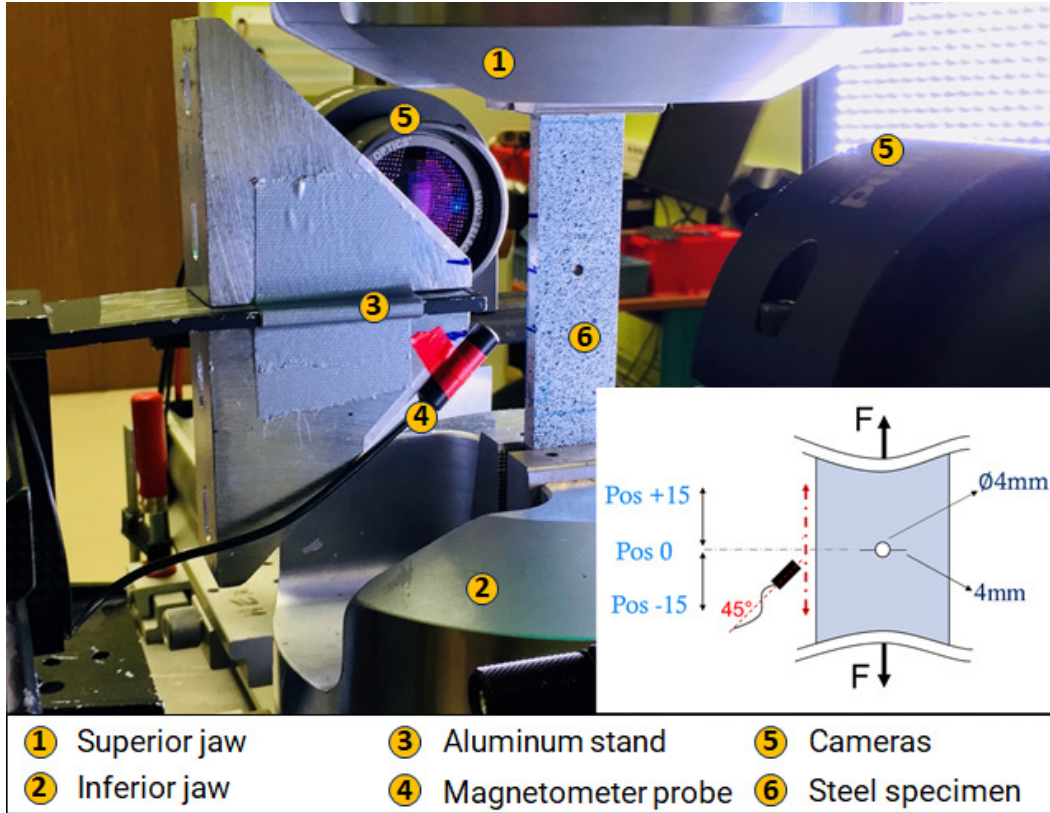


FIG. 2. Experimental setup.

cycles for the last blocks). The range of applied force for this step was [2.7kN - 27kN] using a 4Hz sinusoidal loading.

3-Pictures : After each block, two steps at minimum and maximum force were used to take pictures. The crack tips were calculated by DIC using Correli software⁷ using Williams's series.

B. Experimental results and discussion

Figure 4 illustrates some piezomagnetic loops measured at the three positions during the test. In order to facilitate the comprehension of the figures and the comparison between piezomagnetic loops, the magnetic state at 0kN was considered as a reference state for magnetization, given that the magnetic flux leakage remains a relative measurement.

The loop flux-force changes its shape with the increase of fatigue cycles. Evidently the magnetic signals have a complicated structure and potentially convey more information concerning fatigue-induced changes in the material. The significance of the magnetic signal changes depends on the measurement position. As we can observe the loops recorded at -15mm position exhibit a

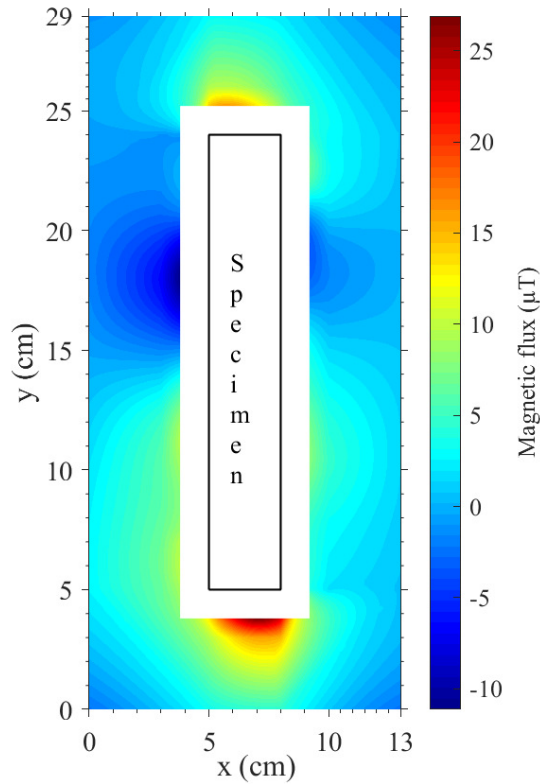


FIG. 3. The variations of the magnetic field measured at 45° depending on the position relative to the specimen.

very important transformation of their shape. A particularly interesting change observed is that the Villari reversal which occurs at a local optimum (maximum or minimum) of the piezomagnetic loop. As the number of fatigue cycles increases, the more the alterations in the magnetic response is important: the Villari reversal shifts to a higher force value and a crossing point of the two halves of the piezomagnetic loop appears. These changes were also observed in the piezomagnetic loops measured at positions 0mm and +15mm but with a smaller breadth. However, the signal remains sensitive to the fatigue process at this positions. There is no direct connection between the material damage and the piezomagnetic hysteresis as is the case for stress-strain loops (their areas have the dimensions of energy density). This is due to the fact that there is no direct link between the two plotted quantities (magnetic flux and mechanical force). However, given the close link between magnetization and microstructural changes in the material and since the area of a loop is one of the most rudimentary indices of its shape, it seems to be useful to try to assess the state of damage of the material. Figure 5 shows the calculated B field-force hysteresis loop areas and the cracks

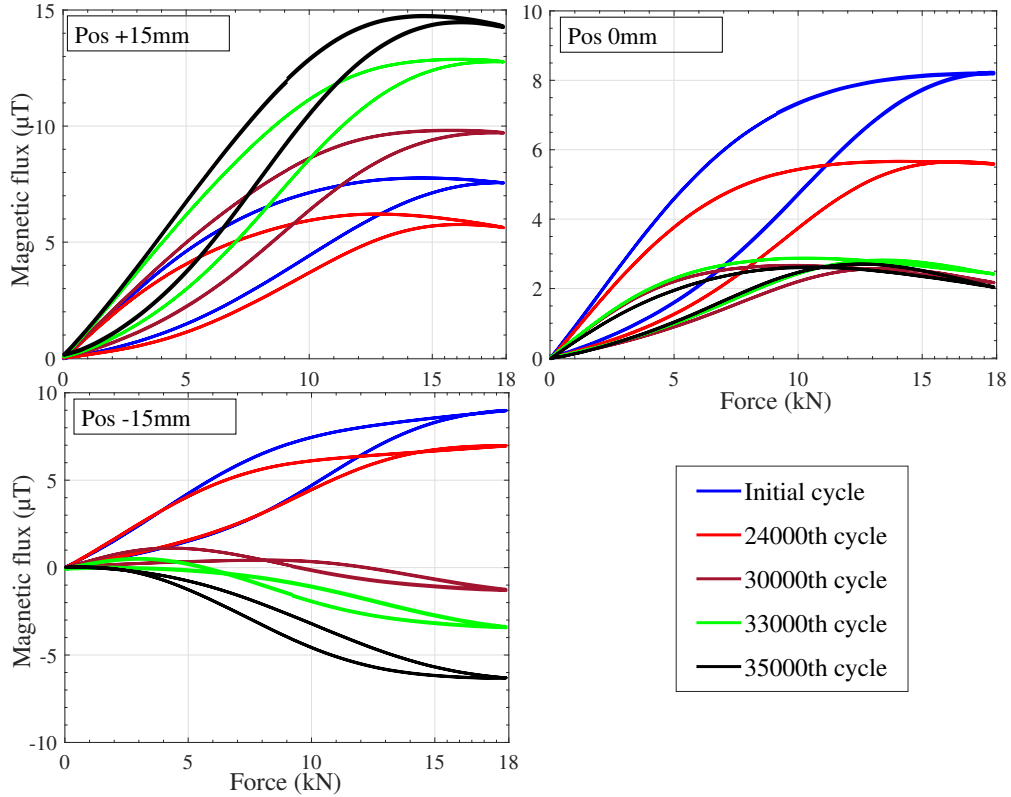


FIG. 4. Some piezomagnetic loops measured during the test at three different positions (-15mm, 0mm and +15mm).

length plotted as a function of the number of fatigue cycles. A strong correlation between the variations was observed. Indeed, the cracks growth leads to a decrease in the active section of the specimen and consequently a considerable increase in the effective stress in the material which modified significantly the magnetic flux.

III. MODELING ASPECTS : MULTISCALE MODELING

The model is derived from a description of reversible magneto-elastic behavior^{8,9} extended recently to magnetic hysteresis¹⁰. This description relies on the definition of the material Gibbs free energy at the magnetic domain scale and the estimation of magnetic domains volume fraction using a *at equilibrium* stochastic approach at the grain scale. Some scale transition rules are used to define the behavior at the polycrystalline scale considered as the representative volume element (*RVE*).

The reader can find complete and comprehensive explanation and hypotheses about the con-

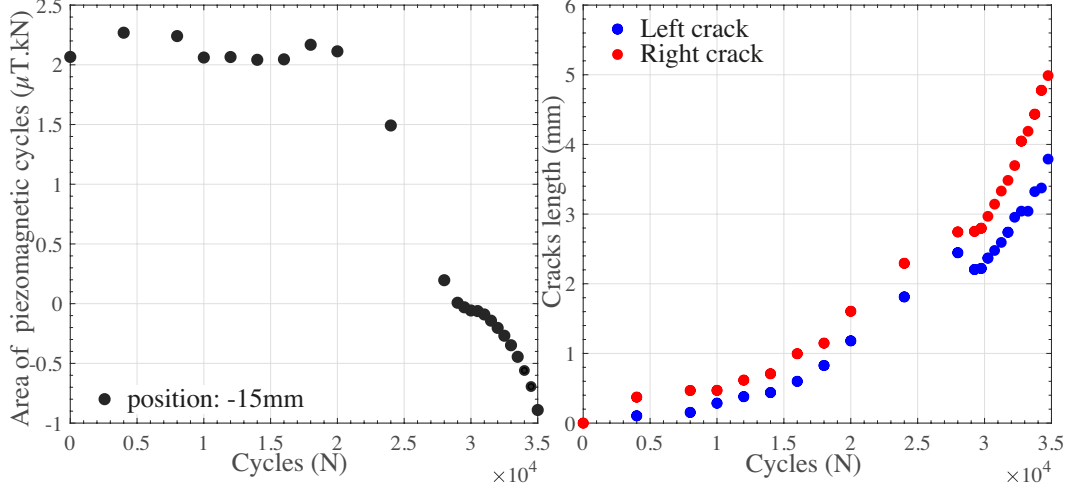


FIG. 5. Evolution of the area of the piezomagnetic loops and the cracks length with the number of cycles.

struct of this energy functional in earlier publications⁹. Indeed at the magnetic domain scale α , both magnetization $\vec{\mathbf{M}}_\alpha$ and magnetostriction strain ϵ_α^μ (seen as a free deformation tensor) can be considered as homogeneous. Following these simplifications, the Gibbs free energy density is simply expressed as:

$$\begin{aligned} \mathfrak{g}_\alpha(\vec{\mathbf{H}}, \boldsymbol{\sigma}) = & K_1(\gamma_{\alpha 1}^2 \gamma_{\alpha 2}^2 + \gamma_{\alpha 2}^2 \gamma_{\alpha 3}^2 + \gamma_{\alpha 3}^2 \gamma_{\alpha 1}^2) - \mu_0 \vec{\mathbf{H}} \cdot \vec{\mathbf{M}}_\alpha \\ & - \frac{1}{2} \boldsymbol{\sigma} : \mathbb{C}^{-1} : \boldsymbol{\sigma} - \boldsymbol{\sigma} : \epsilon_\alpha^\mu \end{aligned} \quad (1)$$

with K_1 the first magnetocrystalline constant, $\gamma_{\alpha i}$ the direction cosines of the local magnetization vector ($\vec{\mathbf{M}}_\alpha = M_s \gamma_{\alpha i} \vec{\mathbf{e}}_i$ with M_s the saturation magnetization and $\vec{\mathbf{e}}_i$ the canonical cubic basis), μ_0 the vacuum magnetic permeability, $\vec{\mathbf{H}}$ the magnetic field (homogeneous over the RVE), $\boldsymbol{\sigma}$ the stress tensor (homogeneous over the RVE) and \mathbb{C} the stiffness tensor of the medium. Magnetostriction strain tensor ϵ_α^μ is defined by:

$$\epsilon_\alpha^\mu = \frac{3}{2} \begin{pmatrix} \lambda_{100}(\gamma_{\alpha 1}^2 - \frac{1}{3}) & \lambda_{111} \gamma_{\alpha 1} \gamma_{\alpha 2} & \lambda_{111} \gamma_{\alpha 1} \gamma_{\alpha 3} \\ \lambda_{111} \gamma_{\alpha 1} \gamma_{\alpha 2} & \lambda_{100}(\gamma_{\alpha 2}^2 - \frac{1}{3}) & \lambda_{111} \gamma_{\alpha 2} \gamma_{\alpha 3} \\ \lambda_{111} \gamma_{\alpha 1} \gamma_{\alpha 3} & \lambda_{111} \gamma_{\alpha 2} \gamma_{\alpha 3} & \lambda_{100}(\gamma_{\alpha 3}^2 - \frac{1}{3}) \end{pmatrix} \quad (2)$$

with λ_{100} and λ_{111} the so-called magnetostriction constants. Calculation of magnetic domains volume fraction is made possible by using a *at equilibrium* stochastic approach, which neglects

the transition zones (domain walls) between domains. This calculation is complemented by a minimization process of g_α regarding the direction cosines of domain families α to take the so-called magnetization rotation mechanism into account. Following this strategy, a Boltzmann function gives the solution of the stochastic approach¹¹ (with V_0 a reference microscopic volume, k_B the Boltzmann constant ($1.38 \times 10^{-23} \text{J.K}^{-1}$) and T the temperature (293K)).

$$f_\alpha = \frac{\exp\left(-\frac{V_0}{k_B T} g_\alpha\right)}{\sum_{\alpha=1}^6 \exp\left(-\frac{V_0}{k_B T} g_\alpha\right)} \quad (3)$$

$$\vec{\gamma}_\alpha = \min(g_\alpha(\vec{\mathbf{H}}, \boldsymbol{\sigma})) \quad (4)$$

Averaging operations end the process as expressed in equations (5), with N_g the number of grains g involved in the process.

$$\vec{\mathbf{M}} = \frac{1}{N_g} \sum_g \left(\sum_{\alpha=1}^6 f_\alpha \vec{\mathbf{M}}_\alpha \right) \quad \epsilon^\mu = \frac{1}{N_g} \sum_g \left(\sum_{\alpha=1}^6 f_\alpha \epsilon_\alpha^\mu \right) \quad (5)$$

A. Irreversible modeling - application of Hauser's modeling to Piezomagnetic loop

An extension of Hauser's model¹² to the piezomagnetic hysteresis has recently been proposed by adding an irreversible contribution $\boldsymbol{\sigma}_{irr}$ to the reversible mechanical stress $\boldsymbol{\sigma}_{rev}$ ⁶.

$$\boldsymbol{\sigma} = \boldsymbol{\sigma}_{rev} + \boldsymbol{\sigma}_{irr} \quad (6)$$

with $\boldsymbol{\sigma}_{rev}$ the *reversible* stress leading to the at equilibrium magnetization using the multiscale model. $\boldsymbol{\sigma}_{irr}$ is given by:

$$\boldsymbol{\sigma}_{irr} = \delta \left(\boldsymbol{\sigma}_c + a' |\boldsymbol{\sigma}_{rev}| \right) \left[1 - \kappa' \exp\left(-\frac{k'_a}{\kappa'} |\boldsymbol{\epsilon}^\mu - \boldsymbol{\epsilon}_{prev}^\mu| \right) \right] \quad (7)$$

and

$$\kappa' = 2 - \kappa'_0 \exp\left(-\frac{k'_a}{\kappa'_0} |\boldsymbol{\epsilon}^\mu - \boldsymbol{\epsilon}_{prev}^\mu| \right) \quad (8)$$

With $\boldsymbol{\sigma}_c$, and parameters a' , k'_a and κ'_0 are four more adjustment parameters. An inversion of loading direction (leading to a change of the sign of parameter δ) is defined as a change of sign for the time derivative of the applied stress.

B. Modeling results and discussion

Physical constants of pure iron have been used for the anhysteretic parameters. All parameters are gathered in Table.I. An orientation data file made of 440 orientations has been used to model the RVE⁶.

TABLE I. Parameters used in the multiscale modeling.

-	M_s	K_1	$\lambda_{100} ; \lambda_{111}$	V_0	σ_c	a'	k'_a	κ'_0
Value	1.71×10^6	48	21.5 ; -21.5	8000	123	0.0	1.3×10^6	1
Unit	A/m	kJ/m ³	ppm	nm ³	MPa	-	-	-

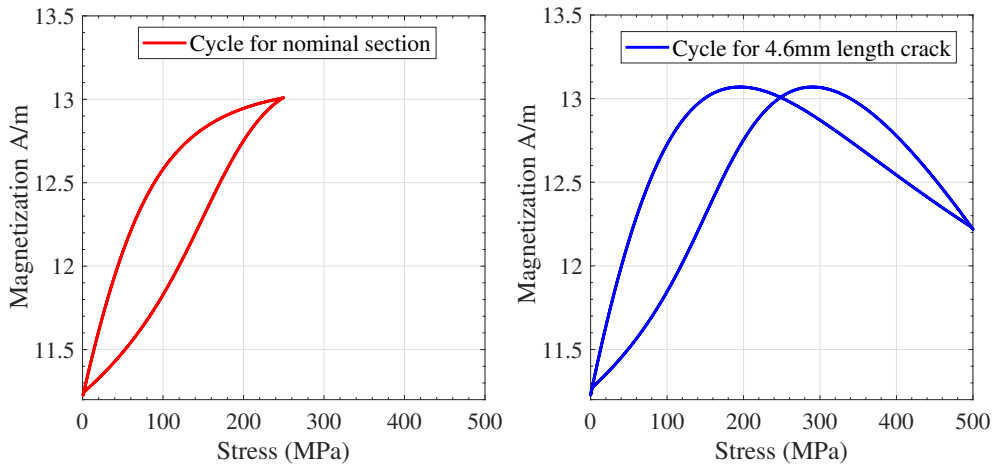


FIG. 6. Piezomagnetic loops calculated by the multiscale model ($H=10\text{mA/m}$).

Thanks to this modeling strategy the piezomagnetic irreversibility was reproduced. Figure 6 presents two piezomagnetic loops calculated for a small magnetic field of about 10 mA/m and different stress conditions corresponding to a nominal loading of a virgin material and after a crack propagation of 4.6mm length respectively. The mechanical state close to the damaged zone is of course very complex with plastic straining, residual stress and singular stress field. The modeling of the effect of these mechanical fields on the magnetic behavior is still not reachable. A possible first approach is to consider a global geometric effect associated with the reduction of ligament. Therefore, the stress is considered homogeneous in the remaining section of matter and the model only takes into account the increase of average stress with crack propagation. The

loops reproduced by the model show a good general agreement with the experimental observations (figure 4): shift of Villari reversal point and piezomagnetic loops cross point. Of course stress concentration and residual stress associated with local plastic strain should be considered.

IV. CONCLUSION

This study is the first insight into a passive piezomagnetic monitoring technique to detect the early stages of fatigue crack growth. Experimental results are consistent with former results performed with low carbon steels. They highlight the effect of fatigue damage on the magnetization of the material seen through the magnetic flux leakage. A multiscale modeling has been used to calculate the piezomagnetic loops. It should be emphasized that the model calculates the magnetic behavior inside of the material while the experimental measurements concern the detection of the variations of one component of the magnetic flux leakage in the air. This is the reason why we cannot make a direct comparison between experimental and modeling results. It should be noted that fatigue damage is too complex to be described simply by scalar variables (one component). It would be interesting to consider the vector variations of the B-field and to develop structural model to better describe the changes in the flux around the specimen.

V. ACKNOWLEDGMENTS

This research was financially supported by Air Liquide R&D, France as part of a CIFRE-partnership with the Laboratory of Mechanics and Technology (LMT), ENS Paris-Saclay and ESILV.

VI. DATA AVAILABILITY

The data that support the findings of this study are available from the corresponding author upon reasonable request.

REFERENCES

- ¹R. M. Bozorth, “Ferromagnetism,” New York : Ed. Van Nostrand (1951).

- ²L. Lolloz, S. Pattofatto, and O. Hubert, “Application of piezomagnetism for the measurement of stress during an impact,” *J. Electrical Engineering* **51 8**, 15–20 (2006).
- ³O. Hubert and K. J. Rizzo, “Anhyseretic and dynamic piezomagnetic behavior of a low carbon steel,” *J. Magnetism and Magnetic Materials* **320 20**, 979–982 (2008).
- ⁴S. Bao, T. Erber, S. A. Guralnick, and W. L. Jin, “Fatigue, magnetic and mechanical hysteresis,” *Strain* **47(4)**, 372–381 (2011).
- ⁵S. A. Guralnick, S. Bao, and T. Erber, “Piezomagnetism and fatigue: II,” *J. Appl. Phys* **41 115006**, 11 (2008).
- ⁶A. Ouaddi, O. Hubert, J. Furtado, D. Gary, and S. Depeyre, “Piezomagnetic behavior: experimental observations and multiscale modeling,” *Mechanics & Industry* **19 6**, 1549–1560 (2020).
- ⁷S. Roux, J. Réthoré, and F. Hild, “Digital image correlation and fracture: an advanced technique for estimating stress intensity factors of 2d and 3d cracks,” *J Phys D Appl Phys* (2009).
- ⁸L. Daniel, O. Hubert, N. Buiron, and R. Billardon, “Reversible magneto-elastic behavior: a multiscale approach,” *Journal of the Mechanics and Physics of Solids* **56**, 1018–1042 (2008).
- ⁹O. Hubert, “Multiscale magneto-elastic modeling of magnetic materials including isotropic second order stress effect,” *Journal of Magnetism and Magnetic Materials* **491**, 1–16 (2019), 165564.
- ¹⁰L. Daniel, M. Rekik, and O. Hubert, “A multiscale model for magneto-elastic behaviour including hysteresis effects,” *Archive of Applied Mechanics* **84 9**, 1307–1323 (2014).
- ¹¹X. Chang, K. Lavernhe, and O. Hubert, “Stochastic multiscale modeling of the thermomechanical behavior of polycrystalline shape memory alloys,” *Mechanics of Materials* **144**, 1–27 (2020), 103361.
- ¹²F. Mballa-Mballa, O. Hubert, S. Lazreg, and P. Meilland, “Multidomain modelling of the magneto-mechanical behaviour of dual-phase steels,” 18th WCNDT - World Conference on Nondestructive Testing, Durban (South Africa) (2012).